Reducing TMPRSS6 ameliorates hemochromatosis and β-thalassemia in mice

Shuling Guo,[1] Carla Casu,[2] Sara Gardenghi,[2] Sheri Booten,[1] Mariam Aghajan,[1] Raechel Peralta,[1] Andy Watt,[1] Sue Freier,[1] Brett P. Monia,[1] and Stefano Rivella[2,3]

[1]Isis Pharmaceuticals, Carlsbad, California, USA. [2]Weill Cornell Medical College, Department of Pediatrics, Division of Hematology-Oncology, New York, New York, USA. [3]Weill Cornell Medical College, Department of Cell and Development Biology, New York, New York, USA.

β-Thalassemia and HFE-related hemochromatosis are 2 of the most frequently inherited disorders worldwide. Both disorders are characterized by low levels of hepcidin (*HAMP*), the hormone that regulates iron absorption. As a consequence, patients affected by these disorders exhibit iron overload, which is the main cause of morbidity and mortality. HAMP expression is controlled by activation of the SMAD1,5,8/SMAD4 complex. TMPRSS6 is a serine protease that reduces SMAD activation and blocks HAMP expression. We identified second generation antisense oligonucleotides (ASOs) targeting mouse *Tmprss6*. ASO treatment in mice affected by hemochromatosis (*Hfe*$^{-/-}$) significantly decreased serum iron, transferrin saturation and liver iron accumulation. Furthermore, ASO treatment of mice affected by β-thalassemia (*HBB*$^{th3/+}$ mice, referred to hereafter as *th3/+* mice) decreased the formation of insoluble membrane-bound globins, ROS, and apoptosis, and improved anemia. These animals also exhibited lower erythropoietin levels, a significant amelioration of ineffective erythropoiesis (IE) and splenomegaly, and an increase in total hemoglobin levels. These data suggest that ASOs targeting *Tmprss6* could be beneficial in individuals with hemochromatosis, β-thalassemia, and related disorders.

Introduction

Iron metabolism is a complex and tightly controlled process due to the important role of iron in cellular and systemic physiology and its potential to cause toxicity. On one hand, iron is important in basic cellular mechanisms, such as erythropoiesis and host-defense mechanisms (1–3). On the other hand, an excess of iron can lead to profound cellular and organ damage (1–3). Thus, it is not surprising that iron absorption can be profoundly altered by different physiological conditions, such as changes in dietary iron intake, inflammation, and anemia (4). The liver hormone hepcidin plays a central role in iron metabolism (5–8). Hepcidin (Hamp) targets ferroportin, the only known iron export protein, which is mainly expressed in enterocytes, macrophages, and hepatocytes, controlling, respectively, iron absorption, recycling, and storage (9). At the molecular level, *Hamp* expression is controlled by the activation of the SMAD1,5,8/SMAD4 complex, which in turn is triggered by the association between the BMP6 ligand, whose expression is proportional to intracellular hepatic iron concentrations, and the BMP-receptor complex (10–12). Hemojuvelin (HJV) acts as a coreceptor and is required to fully activate the SMAD pathway (10, 13–15). In contrast, TMPRSS6 or Matriptase-2, a transmembrane serine protease, cleaves HJV, reducing the phosphorylation of the SMAD complex and attenuating *HAMP* expression (16–20). The fundamental antagonistic roles of *HJV* and *TMPRSS6* on *HAMP* expression are underscored by the observation that patients and mice with mutations affecting one of these 2 genes are, respectively, affected by juvenile hemochromatosis and iron-refractory iron deficiency anemia (IRIDA) (13, 18).

In the liver, additional membrane-associated proteins, including HFE, have been involved with the activation of regulatory pathways that control *HAMP* expression in response to serum iron levels (21). Mutations in the *HFE* gene are associated with the most frequent form of hereditary hemochromatosis, which results from a failure to upregulate *HAMP* and downregulate iron absorption despite an increased iron load (22, 23). HFE-related hemochromatosis, if left untreated, causes abnormal iron deposition in key organs, leading to liver fibrosis, cirrhosis, congestive cardiomyopathy, and diabetes (24).

Forms of anemia combined with active proliferation of erythroid progenitors are characterized by low *HAMP* expression (8). The persistence of the anemia and low expression of *Hamp* are associated with iron overload, such as in β-thalassemia intermedia. In this case, patients do not require blood transfusion for survival, but exhibit increased iron absorption and iron overload due to ineffective erythropoiesis (IE) and suppression of *HAMP*. This condition has been defined as nontransfusion-dependent thalassemia (NTDT) in humans, and recently, has been recognized as one of the most frequent forms of β-thalassemia (8, 25). Iron overload is the most common cause of morbidity and mortality in NTDT patients. The *Hbb*$^{th3/+}$ mouse model (referred to hereafter as *th3/+*) mimics NTDT conditions, showing IE (26). IE is characterized by increased proliferation and decreased differentiation of the erythroid progenitors, apoptosis of erythroblasts due to the presence of toxic hemichromes, reticulocytosis, shorter life span of rbc in circulation, splenomegaly, extramedullary hematopoiesis, and anemia (27, 28). We previously demonstrated that the iron absorbed by *th3/+* mice is excessive relative to the amount of iron needed to maintain hemoglobin (Hb) levels that are reduced compared with those in WT mice (26, 29). Furthermore, analysis of transgenic *th3/+* mice overexpressing *Hamp* indicated that these animals exhibited not only reduced organ iron overload, but also a remarkable amelioration of their anemia and IE (29). This

Authorship note: Shuling Guo, Carla Casu, Brett P. Monia, and Stefano Rivella contributed equally to this work.

Conflict of interest: Shuling Guo, Sheri Booten, Mariam Aghajan, Raechel Peralta, Andy Watt, Sue Freier, and Brett P. Monia are employees and stockholders of Isis Pharmaceuticals. Stefano Rivella receives research support from Isis Pharmaceuticals.

Citation for this article: *J Clin Invest.* 2013;123(4):1531–1541. doi:10.1172/JCI66969.

approach suggested that development of new pharmacological agents to increase *HAMP* expression could be extremely valuable in treating this disorder (30).

Due to the important role of TMPRSS6 in suppressing *HAMP*, it was determined whether the increased expression of *Hamp* observed in *Tmprss6*$^{-/-}$ mice could be beneficial in animals affected by both hemochromatosis and β-thalassemia. In fact, lack of *Tmprss6* in mice affected by hereditary hemochromatosis (*Tmprss6*$^{-/-}$ *Hfe*$^{-/-}$) exhibited an improved iron overload phenotype (31). Furthermore, lack of a functional *Tmprss6* significantly improved iron overload and anemia in *Tmprss6*$^{-/-}$*th3/+* mice (32).

The expression of iron-related genes such as *Id1*, *Atoh8*, *Smad7*, and *Bmp6* are increased in normal animals in response to increased liver iron concentration (LIC) (11, 33). Mouse models of IRIDA have elevated *Id1*, *Smad7*, and *Atoh8* expression, as expected, because the lack of cleavage of Hjv from the plasma membrane of hepatocytes in the absence of *Tmprss6* induces constitutive activation of the BMP/SMAD pathway. *Bmp6*, on the other hand, is unchanged compared with that in normal mice but disproportionately elevated relative to LIC (17, 19, 32). Thalassemic animals (*th3/+*) show normal to increased expression of *Id1*, *Atoh8*, *Smad7*, and *Bmp6* (some differences are seen in males vs. females), although these levels are inappropriately low relative to LIC (32, 34, 35). *th3/+* mice lacking *Tmprss6* (*th3/+Tmprss6*$^{-/-}$) have elevated *Id1*, *Smad7*, and *Atoh8* (32). In the same animals, *Bmp6* expression was slightly decreased (males) or unchanged (females) despite a strong LIC reduction.

In this study, we have examined whether pharmacological reduction of *Tmprss6* expression using antisense technology is an effective approach for the treatment of HFE-related hereditary hemochromatosis and β-thalassemia. Our antisense approach utilized an RNaseH mechanism to degrade the *Tmprss6* RNA species (36). We hypothesized that antisense oligonucleotides (ASOs) targeting *Tmprss6* would reduce *Tmprss6* mRNA and protein levels in the liver and, as a result, increase the expression of *Hamp* to therapeutic levels in these 2 disorders. To this end, we designed and identified potent ASOs against mouse *Tmprss6*. These ASOs significantly reduced *Tmprss6* mRNA in mouse primary hepatocytes ($P < 0.01$). In *Hfe*$^{-/-}$ mice, *Tmprss6*-ASO treatment dramatically decreased serum iron and iron accumulation in the liver. Furthermore, administration of *Tmprss6*-ASO in *th3/+* mice not only reduced serum and liver iron, but also significantly improved anemia ($P < 0.01$).

Results

Tmprss6-ASOs reduced Tmprss6 mRNA in cells. Over 150 ASOs were designed and screened against the mouse *Tmprss6* mRNA transcript. These ASOs were first evaluated in mouse primary hepatocytes for their activity to reduce *Tmprss6* mRNA levels. ASOs were introduced into cells via electroporation, and mRNA levels were determined 16 hours later. Two ASOs, *Tmprss6*-ASO#1 and *Tmprss6*-ASO#2, showed potent reduction of *Tmprss6* mRNA levels in a dose-dependent manner (Figure 1A). The IC_{50}s for these 2 ASOs were 1.2 μM and 1.9 μM, respectively. Both ASOs are complementary to the last exon (exon 18, NM_027902.2) of the mouse *Tmprss6* transcript.

Tmprss6-ASOs reduced Tmprss6 in normal mice and modulated serum iron parameters. To evaluate the activity of *Tmprss6*-ASOs in vivo, ASOs were administered to 6-week-old male C57BL/6 mice at 25, 50, or 100 mg/kg/wk for 4 weeks by twice-a-week subcutaneous injections. Liver *Tmprss6* mRNA levels were significantly reduced in a dose-dependent fashion after treatment ($P < 0.01$). As expected, *Hamp* mRNA levels were dramatically upregulated, also in a dose-dependent manner. An approximately 90% reduction of *Tmprss6* levels was associated with a 4- to 5-fold increase in *Hamp* mRNA levels in the 100 mg/kg treatment group (Figure 1, B and C). These mice were fed with normal chow (Laboratory Rodent Diet 5001) and showed a serum iron concentration of approximately 110 μg/dl and transferrin (Tf) saturation of 35% in the vehicle control group. However, after *Tmprss6*-ASO treatment, there was a significant reduction of serum iron levels and Tf saturation ($P < 0.01$), correlating with the reduction of *Tmprss6* levels and the increase of *Hamp* levels. In both the 100 mg/kg treatment groups, serum iron and Tf saturation were reduced to approximately 40 μg/dl and 10%, respectively (Figure 1, D and E). Furthermore, serum Tf levels increased significantly after ASO treatment, showing a trend that was inversely proportional to serum iron levels (Figure 1F and Supplemental Figure 1A; supplemental material available online with this article; doi:10.1172/JCI66969DS1). As expected, reduction of serum iron parameters was associated with a decrease in Hb and an increase in erythropoietin (Epo) levels (Supplemental Figure 1B and Supplemental Table 1). Both ASOs showed similar pharmacology in normal mice. Similar effects on serum iron and iron Tf were observed in both male and female mice (Supplemental Figure 1, C and D). These data demonstrated that *Tmprss6*-ASOs were potent modulators in vivo to upregulate *Hamp* expression and reduce serum iron availability. A control ASO of the same chemistry as *Tmprss6*-ASO was tested and caused no significant changes in *Tmprss6* or *Hamp* mRNA levels (Supplemental Figure 2, A and B). In addition, proinflammatory-related genes, including IL-6 and serum amyloid P (SAP), showed no significant changes in control ASO or *Tmprss6*-ASO treatment groups (Supplemental Figure 2, C and D), indicating that *Hamp* upregulation was not due to a proinflammatory response to ASOs. Body weights, organ (liver, kidney, and spleen) weights, and histopathology as well as serum transaminases were monitored and showed no significant changes with treatment (data not shown). In conclusion, treatment with *Tmprss6*-ASOs was effective and well tolerated.

Tmprss6-ASO treatment in Hfe$^{-/-}$ *mice reduced liver iron accumulation*. *Hfe*$^{-/-}$ mice show defects in iron-regulated *Hamp* expression due to the lack of *Hfe*, a critical regulator that responds to increased iron absorption and iron overload. *Hfe*$^{-/-}$ mice, therefore, mimic human HFE-related hemochromatosis. These mice demonstrate higher dietary iron absorption, which leads to iron overload in the liver. To test the effect of *Tmprss6* reduction in these mice, *Tmprss6*-ASO#2 was administered to a cohort of male and female *Hfe*$^{-/-}$ mice (9 to 13 weeks of age) at 100 mg/kg/wk for 6 weeks. After treatment of *Hfe*$^{-/-}$ mice with *Tmprss6*-ASO, an approximately 90% reduction of *Tmprss6* was observed in the livers of both sexes, while *Hamp* was upregulated 3.1- and 1.7-fold, respectively, in males and females (Figure 2, A and B). Liver TMPRSS6 protein was dramatically reduced after treatment, confirming the mRNA results (Supplemental Figure 3A and ref. 37). As a result, in both sexes, serum iron levels were reduced from more than 300 μg/dl to less than 150 μg/dl, and Tf saturation was reduced from greater than 90% to less than 25% (Figure 2, C and D). Serum iron and Tf saturation were similar to or even lower than the values observed in untreated C57BL/6 mice (Figure 1, D and E). These reductions in serum iron parameters were also reflected in tissue iron accumulation. There was a significant reduction of LIC in the ASO treatment group compared with the vehicle control group, with about 40% reduction in male mice and 30% in female mice (Figure 2E). Conversely, spleen iron concentration was increased in the ASO treatment

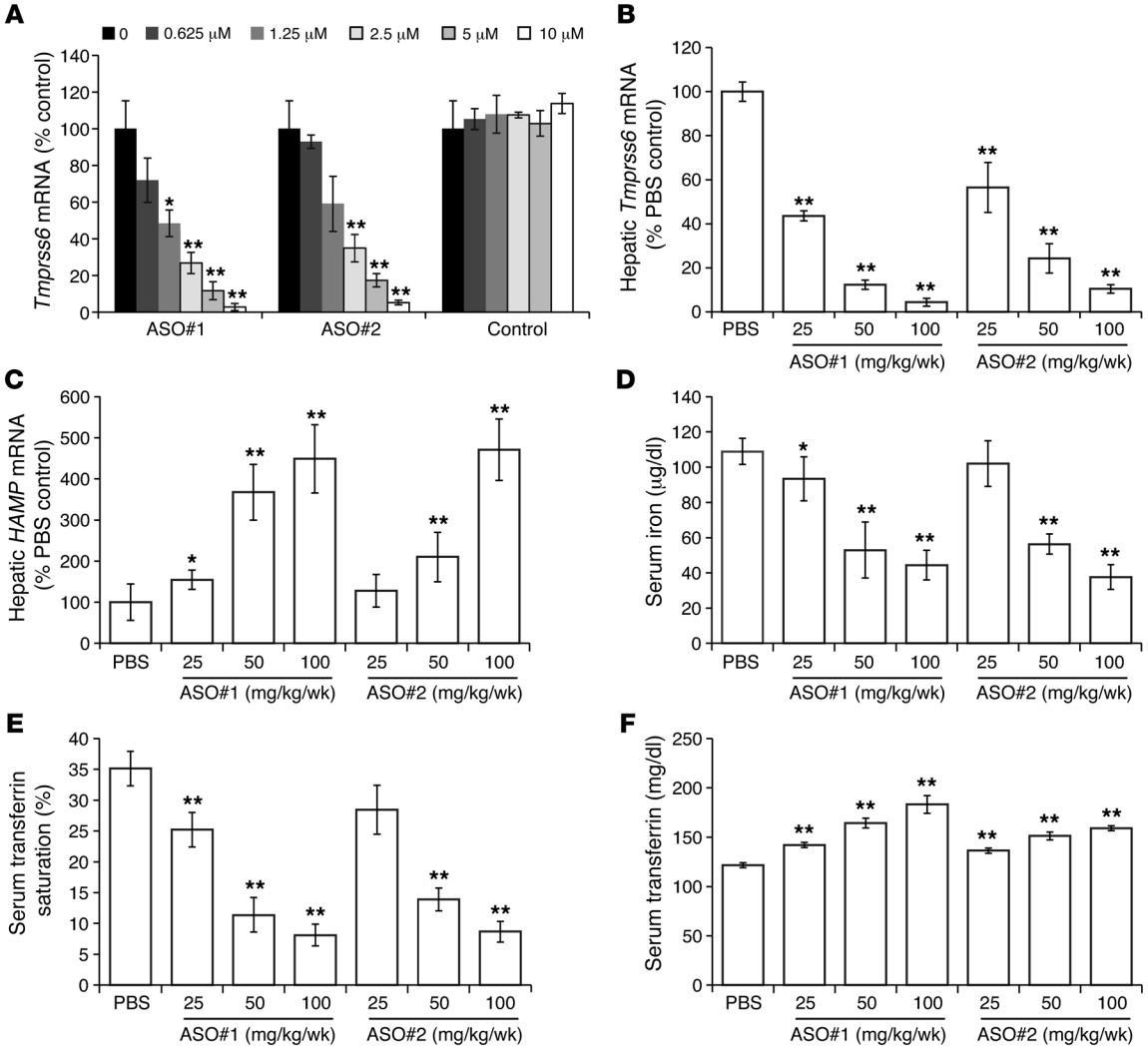

Figure 1

Characterization of *Tmprss6*-ASOs that effectively reduce *Tmprss6* levels in cells and in normal mice. (**A**) Dose-dependent reduction of *Tmprss6* mRNA in mouse primary hepatocytes. Results represent mean ± SD ($n = 2$) compared with untransfected control (UTC). (**B**) Dose-dependent reduction of mouse *Tmprss6* mRNA levels in C57BL/6 mice after *Tmprss6*-ASO treatment. (**C**) Dose-dependent upregulation of liver HAMP levels after *Tmprss6*-ASO treatment. (**D**) Dose-dependent reduction of serum iron levels after *Tmprss6*-ASO treatment. (**E**) Dose-dependent reduction of serum Tf saturation after *Tmprss6*-ASO treatment. (**F**) Serum Tf levels. Six-week-old C57BL/6 male mice were treated for 4 weeks with the indicated doses in mg/kg/wk of *Tmprss6*-ASO via subcutaneous injection. Mouse *Tmprss6* and *HAMP* mRNA levels in liver were quantified by qRT-PCR (TaqMan), and serum iron parameters were determined on a Beckman Coulter clinical analyzer. Results represent mean ± SD ($n = 4$). $^*P < 0.05$; $^{**}P < 0.01$ by Student's *t* test.

groups, with an approximately 80% increase in males and 40% in females (Figure 2F). These observations were confirmed by Pearl's Prussian blue staining, which showed that levels of liver iron were reduced, while iron levels were increased in spleen due to sequestration in macrophages after ASO treatment (Figure 2G). Similarly to what was observed in WT mice after ASO treatment, serum Tf concentration and Epo levels increased as the serum iron levels decreased (Figure 2H and Supplemental Figure 3B). Complete blood count (CBC) analysis indicated that *Tmprss6*-ASO treatment induced a reduction in rbc counts, Hb, and hematocrits. However, all of these parameters were moderately reduced or in the normal range (Supplemental Table 1). *Hfe*$^{-/-}$ mice were also treated with *Tmprss6*-ASO#1, yielding similar pharmacology (data not shown). ASO treatment was well tolerated in *Hfe*$^{-/-}$ mice, and no abnormal findings were observed. These data indicated that *Tmprss6*-ASO treatment decreased iron absorption and, concurrently, redistributed iron from parenchymal cells to macrophages.

Tmprss6-ASO treatment reduced serum iron parameters and liver iron overload in th3/+ mice. Five-month-old *th3/+* mice, both males and females, were treated with *Tmprss6*-ASO for 6 weeks. In both sexes, approximately 85% *Tmprss6* reduction was associated with a modest but significant increase in absolute *Hamp* expression (Figure 3, A and B). Furthermore, when the expression levels of *Hamp* levels were normalized to the LIC, the difference was even more significant, corresponding to a 3.4- and 2.0-fold increase, respectively, in males and females (Figure 3C). ASO treatment significantly

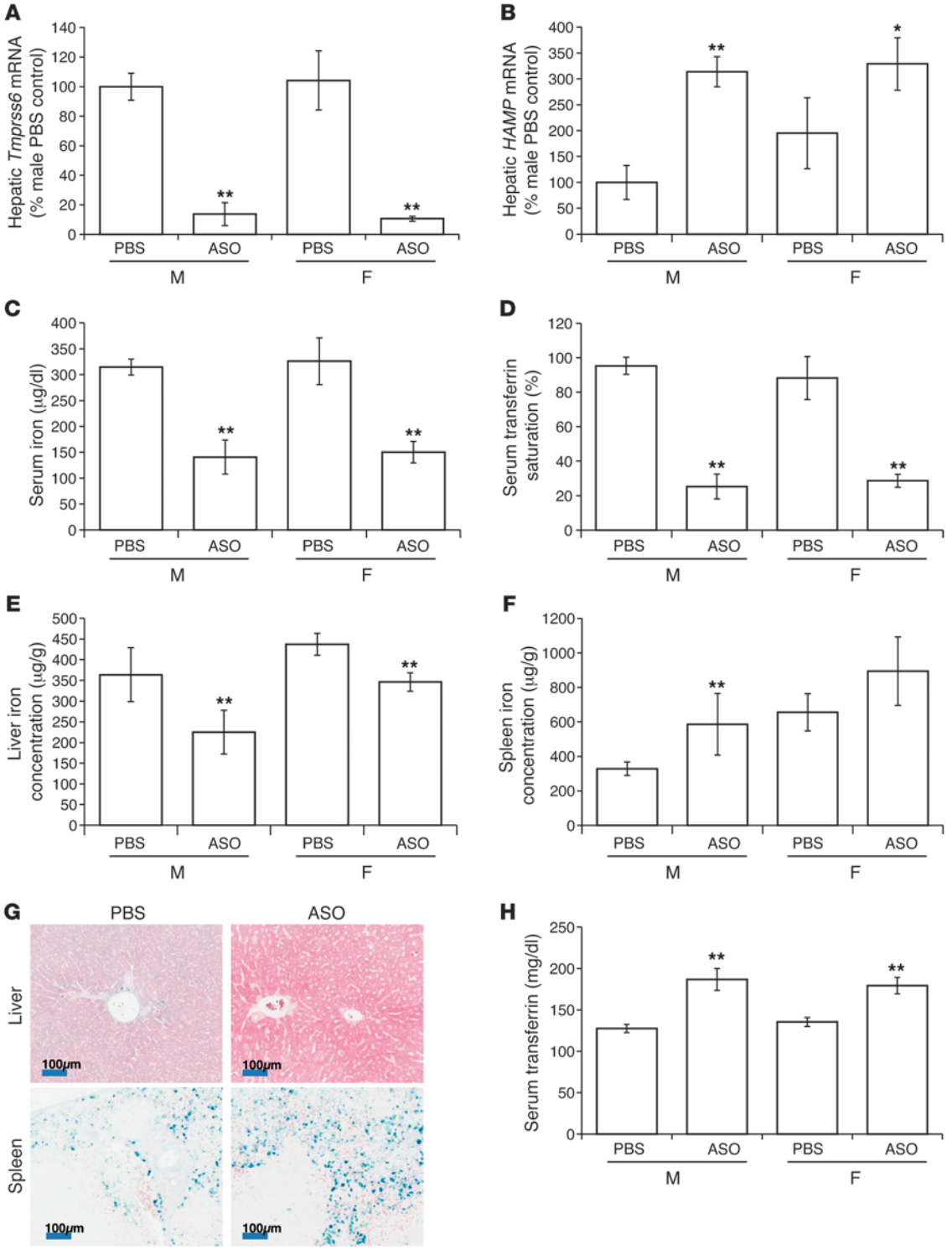

Figure 2

Tmprss6-ASO treatment in *Hfe*$^{-/-}$ mice reduced iron overload. (**A**) Liver *Tmprss6* mRNA levels. (**B**) Liver *Hamp* mRNA levels. (**C**) Serum iron levels. (**D**) Serum Tf saturation. (**E**) LIC. (**F**) Spleen iron concentration. (**G**) Iron stain in the liver and spleen (Pearl's Prussian blue). (**H**) Serum Tf levels. 9- to 13-week-old *Hfe*$^{-/-}$ mice were treated with 100 mg/kg/wk for 6 weeks before analysis. Results represent mean ± SD. n = 5 and 6 for male mice in control and treatment groups, respectively; n = 4 and 3 for female mice in control and treatment groups, respectively. *P < 0.05; **P < 0.01 by Student's t test. Scale bars: 100 μm.

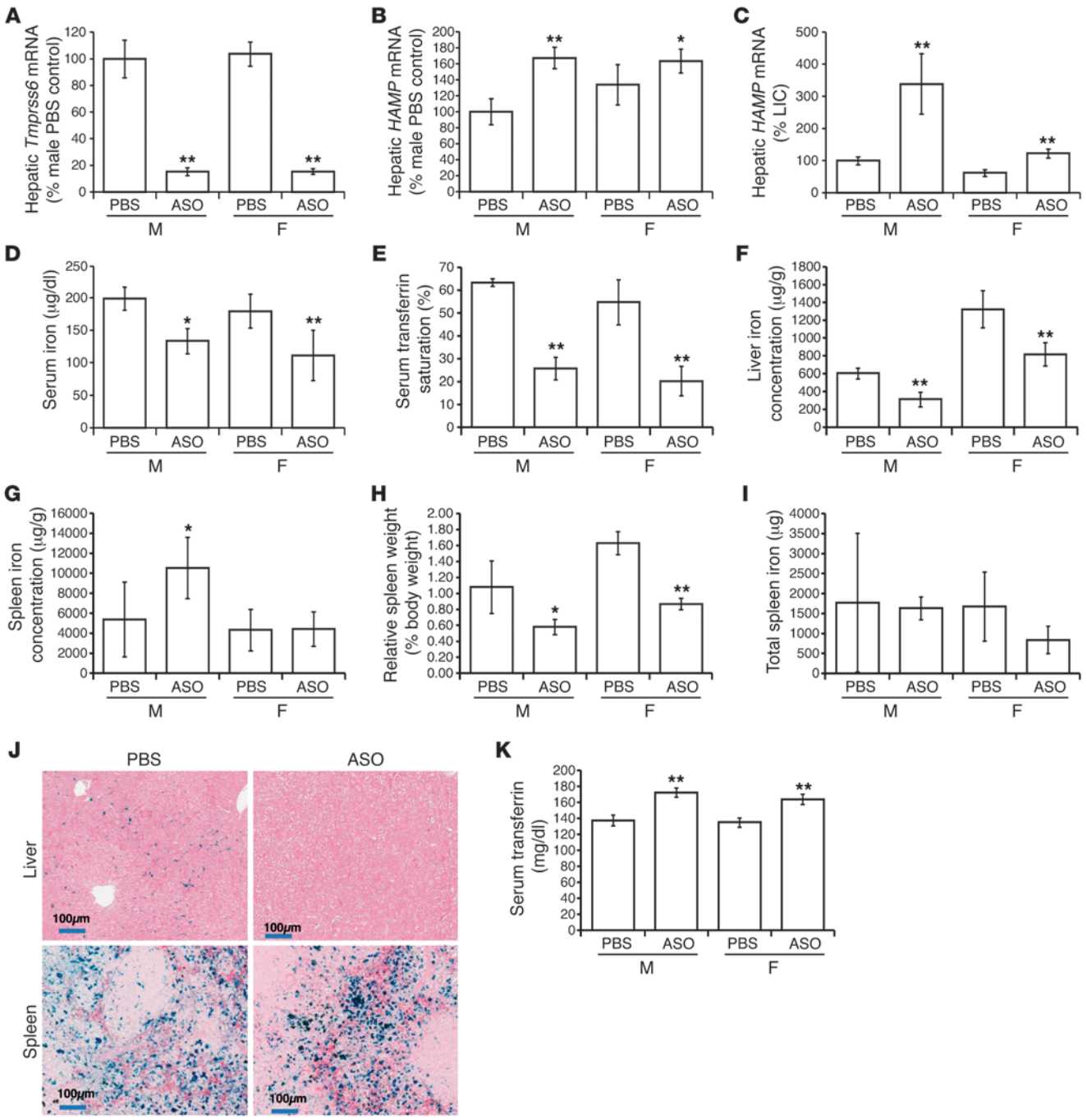

Figure 3

Tmprss6-ASO treatment in *th3*/+ mice reduced iron overload. (**A**) Liver *Tmprss6* mRNA levels. (**B**) Liver *Hamp* mRNA levels, normalized by total RNA. (**C**) Liver *Hamp* mRNA levels, normalized by LIC. (**D**) Serum iron levels. (**E**) Serum Tf saturation. (**F**) LIC. (**G**) Spleen iron concentration. (**H**) Spleen weight normalized by total body weight. (**I**) Total spleen iron. (**J**) Iron stain in the liver and spleen (Pearl's Prussian blue). (**K**) Serum Tf levels. Approximately 5-month-old *th3*/+ mice were treated with 100 mg/kg/wk *Tmprss6*-ASO or PBS for 6 weeks before analysis. Results represent mean ± SD. $n = 4$ for male mice in each group; $n = 4$ and 5 for female mice in control and treatment groups, respectively. $^{*}P < 0.05$; $^{**}P < 0.01$ by Student's t test. Scale bars: 100 μm.

reduced serum iron levels (>30% reduction in both males and females; Figure 3D) and Tf saturation (in *th3*/+ males and females, respectively, from 63% and 55% in control groups to 26% and 20% in treatment groups; Figure 3E). Serum iron and Tf saturation levels were similar to values observed in untreated C57BL/6 mice of similar age and sex (data not shown). LIC was also greatly reduced (50% and 40% reduction, respectively, in males and females; Figure 3F), such that these values were now in the normal range (data not

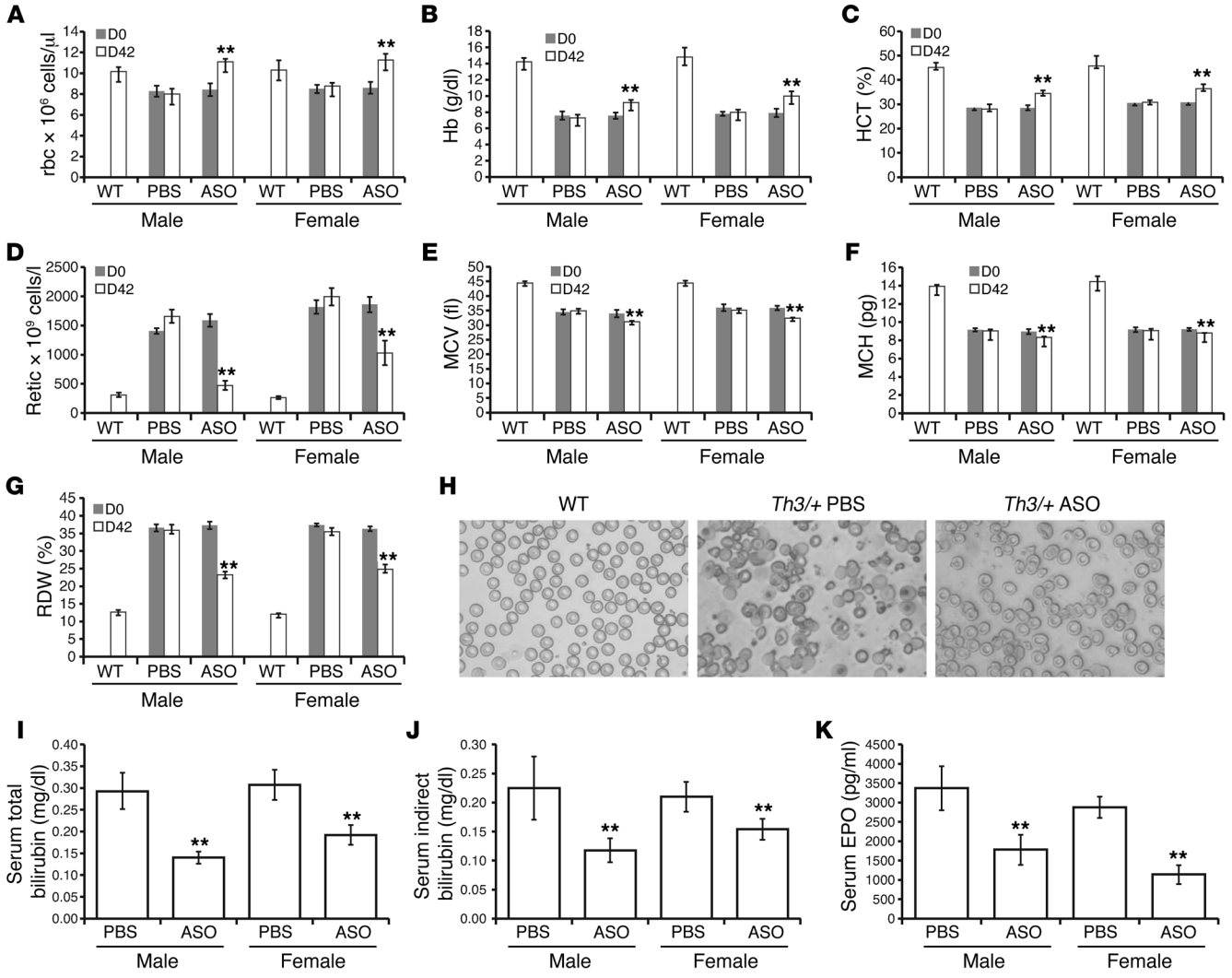

Figure 4

Tmprss6-ASO treatment in *th3*/+ mice improved anemia. (**A**) rbc, (**B**) Hb, (**C**) hematocrit (HCT), (**D**) reticulocytes (retic), (**E**) MCV, (**F**) MCH, and (**G**) RDW in WT and *th3*/+ control or *Tmprss6*-ASO–treated *th3*/+ animals. (**H**) Blood smears and red cell morphology (Giemsa staining). Original magnification, ×40. (**I**) Total and (**J**) indirect bilirubin levels. (**K**) Serum EPO levels. Approximately 5-month-old *th3*/+ mice were treated with 100 mg/kg/wk *Tmprss6*-ASO or PBS for 6 weeks before analysis. Results represent mean ± SD; $n = 4$ for male mice in each group; $n = 4$ and 5 for female mice in control and treatment groups, respectively. $^{*}P < 0.05$; $^{**}P < 0.01$ by Student's t test when treatment group was compared with vehicle control group at the end of treatment.

shown). This difference in LIC indicates a sex effect, as previously reported (32). The concentration of iron in the spleen increased in males (50% higher in treated animals; Figure 3G), while not being modified in females, reflecting again a difference in iron metabolism in males versus females. However, splenomegaly was greatly improved in both male and female treatment groups, as indicated by an approximately 50% reduction of spleen weight (Figure 3H). When the total weight of the spleen was taken into account, the total iron content in the whole organ did not differ between treated and untreated males, while it decreased in treated females (Figure 3I). Overall, these values were 2 to 5 times higher than in normal mice (data not shown). Morphological inspection of the spleen indicated that decreased splenomegaly was associated with improved organ architecture, showing a normalization of the relative proportion between the white and red pulp (data not shown). Furthermore, Pearl's Prussian blue staining indicated that the iron was predominantly localized in macrophages (Figure 3J), as expected with increased *Hamp* expression. Moreover, as seen in WT and *Hfe*$^{-/-}$ mice treated with *Tmprss6*-ASO, serum Tf levels increased as serum iron decreased (Figure 3K). *th3*/+ animals lacking *Tmprss6* expression (*th3*/+*Tmprss6*$^{-/-}$) showed elevated expression of *Id1*, *Smad7*, and *Atoh8*, while *Bmp6* expression was slightly decreased in males or unchanged in females (32). We then investigated whether this was the case in *th3*/+ animals treated with *Tmprss6*-ASO. Our data confirm the trend previously shown by Nai and colleagues (32), with the only exception being *Bmp6*, which in our hands was increased in males and was unchanged in females (Supplemental Figure 4, A–D). These differences might be due to the fact that thalassemic transgenic animals lacking *Tmprss6* exhibit suboptimal levels of iron in their liver, while in our experimental model

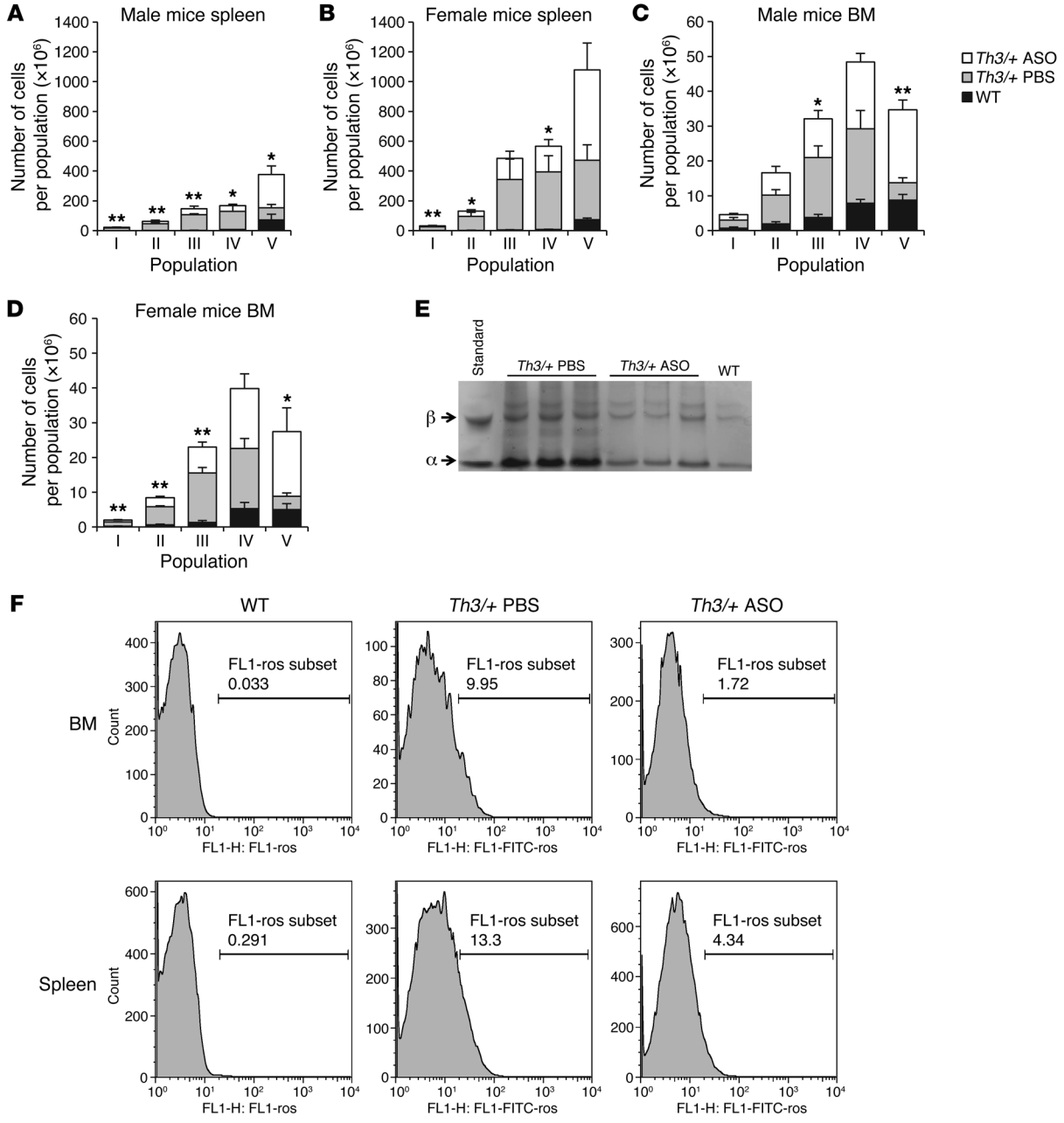

Figure 5

Tmprss6-ASO treatment in *th3*/+ mice improved IE. (**A**) FACS analysis to discriminate different stages of erythroid differentiation in the spleen using the Ter119 and CD44 antibodies. This assay allows the separation of erythroid cells into distinct populations corresponding to proerythroblasts (fraction I), basophilic (II), polychromatic (III), orthochromatic cells, and reticulocytes (IV), and mature rbc (V). Absolute numbers of the different stages of erythroid cells are shown in the spleen in male (**A**) and female mice (**B**) and in the BM in male (**C**) and female mice (**D**). (**E**) TAU gel electrophoresis. (**F**) ROS analysis by FACS, showing a representative sample of the percentage of ROS-positive cells in fraction V. Results represent mean ± SD. $n = 4$ for male mice in each group; $n = 4$ and 5 for female mice in control and treatment groups, respectively. $^*P < 0.05$; $^{**}P < 0.01$ by Student's t test when treatment group was compared with vehicle control group.

the LIC values were in the normal range; it could also be due to the difference in genetic background (C57BL/6 background in this study and mixed background in Nai et al.; ref. 32).

Tmprss6-ASO treatment improved anemia in th3/+ mice. Increased expression of *Hamp* not only reduced tissue iron levels, but also had a beneficial effect on erythropoiesis in *th3*/+ mice. The hematological parameters in the *Tmprss6*-ASO–treated *th3*/+ mice improved compared with those treated with vehicle control. Specifically, anemia end points were significantly improved with ASO treatment in both sexes, including increases in rbc, Hb, and hematocrit (approximately 30%, 2 g/dl, and 20%, respectively; Figure 4, A–C, and Supplemental Table 2). Furthermore, ASO-treated *th3*/+

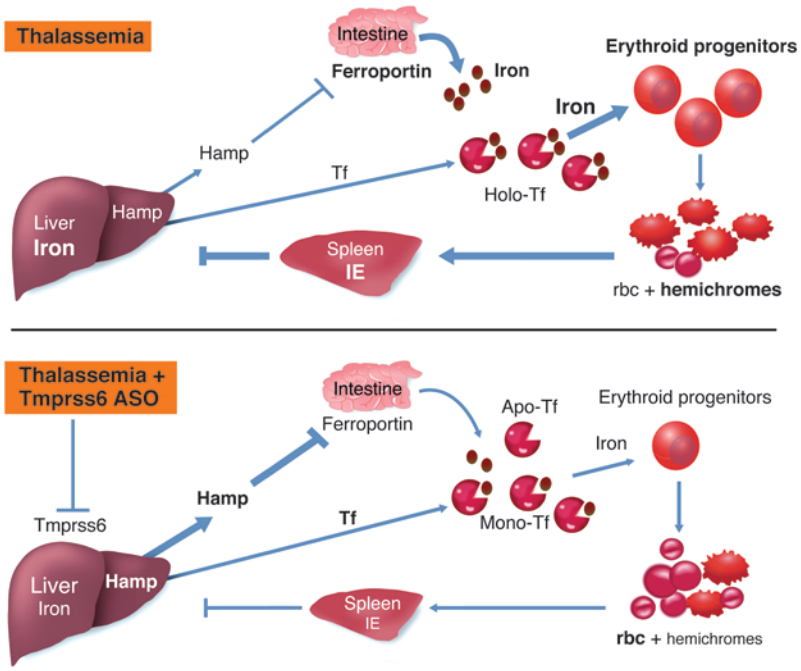

Figure 6
Proposed mechanism for *Tmprss6*-ASO treatment in iron overload and anemia improvement. Apo-Tf, monoferric-Tf and Holo-Tf, respectively, represent empty-, monoferric-, and diferric-loaded Tf (see text for details).

mice exhibited lower reticulocyte numbers, mean corpuscular Hb (MCH), and mean corpuscular volume (MCV) (Figure 4, D–F). The blood smears showed that red cell morphology was significantly improved after ASO treatment (Figure 4H), confirming the reduction of red cell distribution width (RDW) (Figure 4G). In addition, serum total bilirubin was greatly reduced in the ASO treatment group (Figure 4I). Since the majority of the total bilirubin was indirect bilirubin (Figure 4J), this indicated that ASO treatment decreased hemolysis. In *th3/+* mice, ASO treatment significantly reduced EPO values (Figure 4K), further confirming that anemia conditions were improved after treatment. These EPO values were still higher than those in WT animals of similar age and corresponded, on average, to 500 pg/ml in males and 150 pg/ml in females (not shown).

Tmprss6-ASO treatment prevented hemichrome formation and enhanced erythroid differentiation in th3/+ mice. Treatment with *Tmprss6-ASO* significantly ameliorated the IE in *th3/+* mice, as indicated by FACS analysis (Supplemental Figure 5A). Furthermore, while the number of rbc increased with *Tmprss6*-ASO treatment, reticulocyte counts decreased (Figure 4, A and D) as did the percentage and absolute number of immature erythroid progenitor cells in the spleen, and, to a lesser extent, in the BM (Figure 5, A–D). Therefore, ASO treatment improved rbc production and erythroid maturation, the latter demonstrated by a significant normalization in the relative proportion between the number of erythroblasts/reticulocytes and enucleated erythroid cells (Figure 5, A–D). Analysis of the CBC values indicated that *Tmprss6*-ASO–treated *th3/+* animals had reduced MCV and MCH parameters, suggesting, as previously observed (29), that lower Tf saturation levels were associated with decreased erythroid iron intake and hemichrome formation. Improvement in erythropoiesis could then be associated with decreased formation of insoluble globins (α chain/heme aggregates), thereby reducing their potential toxicity when adhering to rbc membranes and producing ROS (29). Analysis of membrane fractions by determining the amount of bound globins by triton acetic acid urea (TAU) gel electrophoresis indicated a significant decrease in the formation of toxic α-globin/heme aggregates (Figure 5E), likely being responsible for the improvement in RDW as well as morphology of the erythrocytes (Figure 4, G and H). Additionally, a ROS indicator, 5-(and -6)-chloromethyl-2′,7′-dichlorodihydrofluorescein diacetate, acetyl ester (CM-H2DCFDA), was added to the spleen and BM cells. This compound permeates into the cells and is oxidized in the presence of ROS or free heme. FACS analysis indicated that mature erythroid cells of *Tmprss6*-ASO–treated *th3/+* mice showed a significant reduction of ROS (Figure 5F). As a result, apoptosis was dramatically decreased with *Tmprss6*-ASO treatment (Supplemental Figure 5B). Increased expression levels of *Id1* and *Gdf15* in erythroid cells have been associated, respectively, with increased survival of erythroid cells and IE (38, 39). In particular, *Id1* expression inversely correlates with *Tmprss6* expression in the liver, while high levels of GDF15 in thalassemic patients have been associated with low levels of hepcidin expression (39, 40). However, in mice, *Tmpress6* is expressed at very low levels in the spleen, while the correlation between expression of *Gdf15* and *Hamp* under conditions of stress erythropoiesis and in IE has not been confirmed (41). Nevertheless, we performed expression analysis of these 2 genes in the spleen of control and *Tmprss6*-ASO–treated *th3/+* mice, observing no significant differences (data not shown). Together, these data support the conclusion that treatment with *Tmprss6*-ASO has an indirect beneficial effect on erythropoiesis through its role on *Hamp* expression and consequent decreased Tf saturation.

Discussion

Iron balance must be carefully regulated to provide iron for essential physiological functions and erythropoiesis while avoiding the toxicity associated with its excess. Tissue iron overload is a primary focus of hemochromatosis and β-thalassemia management. If untreated, iron overload leads to organ failure and death.

The primary cause of iron overload in *HFE*-related hemochromatosis is the inability of patients to respond to increased serum iron

concentration by adjusting *Hamp* levels (24, 42). This is a common genetic disorder in people of Northern European origin, with an estimated prevalence of 1 in 200, where patients are homozygous for the C282Y mutation in *HFE* (24, 42, 43). Without therapeutic intervention, iron overload leads to multiple organ damage, such as liver cirrhosis, cardiomyopathy, diabetes, arthritis, hypogonadism, and skin pigmentation (24). Phlebotomy is the only treatment option, while iron chelation therapies are extremely rare and controversial (44, 45). However, phlebotomy increases erythropoiesis to compensate for blood loss, and Hamp levels are further suppressed by high erythropoietic activity, thereby leading to more dietary iron absorption (23, 46). This may lengthen the duration of the "de-ironing" stage after initial diagnosis of *HFE*-related hemochromatosis, due to very frequent phlebotomies (weekly phlebotomy for 3 months to a year) (47). In this setting, *Tmprss6*-ASO treatment might slow down the intestinal iron absorption, reducing the frequency of phlebotomy and/or shortening "de-ironing" phase. Our data indicate that administration of *Tmprss6*-ASO is efficient in reducing iron overload in *Hfe*$^{-/-}$ mice. This was associated with a moderate decrease in rbc synthesis and Hb levels. However, the low levels of Tf saturation associated with reduced levels of Hb suggest that lower doses of *Tmprss6*-ASO might be sufficient to prevent iron overload or reduce iron absorption following phlebotomy with minimal to no effect on erythropoiesis.

The primary forms of NTDT include β-thalassemia intermedia, Hb E β-thalassemia, and Hb H disease (48). Estimates indicate that approximately 68,000 children are born with various forms of thalassemia each year (48). Roughly 30% of these individuals suffer from β-thalassemia major. In the remaining group of individuals, a smaller but yet ill-defined number have NTDT. Due to limited genetic analyses and clinical experience with this disorder, it is speculated that only a fraction of these individuals are currently diagnosed as having NTDT (49, 50). Recent studies have raised awareness of this condition; therefore, it is expected that a larger number of NTDT patients will be recognized over time. The IE in NTDT patients leads to suppression of *HAMP* and increased iron absorption. Over time, these patients exhibit exacerbated IE and splenomegaly, with a deterioration of many clinical pathological features associated with iron overload. Iron chelators can be used in NTDT patients to treat iron overload, which is induced by IE. This approach relies on removing the excess iron accumulated by increased iron absorption. However, both phlebotomy and iron chelators do not target the mechanism responsible for excessive iron absorption, which is low levels of *HAMP* expression.

Previous studies in mice indicated that excessive *Hamp* production is detrimental (16, 51). However, additional studies have provided evidence that moderate increases in *Hamp* expression or by administration of Hepcidin agonists could be extremely beneficial to prevent excessive iron absorption in models of hemochromatosis and β-thalassemia, emphasizing the fact that a therapeutic benefit would depend upon the level of *Hamp* elevation achieved (29–31). For instance, it has been demonstrated that supply of exogenous Hamp (miniHepcidin) or other Hamp agonists could ameliorate the iron overload in animal models of hemochromatosis (52–54). Additional studies using models of β-thalassemia intermedia that were kept on a low-iron diet, genetically modified to increase *Hamp* expression, including genetic mutations inactivating *Tmprss6*, or through treatment with apo-Tf demonstrated that reducing erythroid iron intake was associated with a significant reduction of splenomegaly and IE and an increase in rbc numbers and Hb levels (29, 32, 55). Together, these observations suggest that lowering Tf saturation levels under conditions of dietary iron restriction will reduce erythroid intake per cell (lower MCH), but increase the number of red cells that will receive iron. The goal might be to keep the production and the number of rbc stable, a process that is likely more efficient and safe than producing fewer rbc, each one with a normal MCH. Therefore, targeting *TMPRSS6* in β-thalassemia might have several positive effects: preventing excessive iron absorption and iron overload, increasing serum Tf concentrations, which will further decrease Tf saturation and hemichrome formation, and safely storing the excess of iron in macrophages. Therefore, development of new strategies to increase *HAMP* expression by modulation of *TMPRSS6* expression might represent the next clinical goal for improving the management of hemochromatosis and β-thalassemic patients.

In NTDT patients, IE triggers many pathophysiological outcomes, including anemia, expansion of the erythron, formation of abnormal rbc, splenomegaly, and decreased HAMP synthesis, which in turn leads to iron overload (Figure 6). Recently, we learned that high levels of Tf saturation and iron delivered to erythroid progenitors are associated with production of hemichromes that negatively affect erythropoiesis (8, 29, 55). As patients age, the size of the spleen increases and sequesters a growing number of rbc. As a consequence, the number of erythroid progenitors expands in an attempt to compensate for the anemia, negatively affecting *HAMP* expression. In this scenario, iron plays a major role in the deterioration of the disease. Based on previous observations and our data, we postulate that increasing *HAMP* expression will not only prevent or reduce iron overload (Figure 6), but will also break this vicious cycle (30). From the prospective of rbc synthesis, *Tmprss6*-ASO–mediated upregulation of *Hamp* is associated with decreased levels of Tf saturation and production of hemichromes, which in turn improve red cell survival and production (Figure 6). In *th3/+* mice, we showed that this is accompanied by decreased Epo levels, a decreased number of erythroid progenitors, and splenomegaly. This, together with the observation that *Id1* expression in the spleen is unchanged, support a mechanism whereby iron effects predominate, rather than a direct *Tmprss6*-ASO effect on erythropoiesis. Therefore, a moderate increase in *Hamp* levels substantially and positively affects multiple features associated with IE and iron overload. If this is also the case in humans, NTDT patients might benefit substantially from this treatment, preventing the need for undesirable treatment regimens such as iron chelation, splenectomy, and eventually, chronic blood transfusion.

Interestingly, in our study, we also observed an inverse correlation between iron and Tf concentrations in the serum of *Tmprss6*-ASO–treated mice, consistent with previous reports demonstrating a negative correlation between iron deficiency and Tf synthesis (56–58). Intriguingly, this suggests that increased serum Tf levels might be utilized as a parameter to predict iron deficiency and evaluate when *Tmprss6*-ASO treatment should be stopped. This hypothesis was supported by the observation that serum Tf in C57BL/6 mice and *Hfe*$^{-/-}$ mice increased on a low-iron diet (Supplemental Figure 6).

In summary, our study demonstrates that targeting *Tmprss6* by antisense technology can modulate *Hamp* expression in a dose-dependent manner, indicating that *Tmprss6*-ASO treatment has the potential to titrate *Hamp* expression to the right amount to prevent iron overload in disorders associated with abnormally low levels of Hamp. This notion is strengthened by our results dem-

onstrating that *Tmprss6*-ASO treatment reduces iron overload in an animal model of hemochromatosis and improves both iron overload and anemia in mice affected by β-thalassemia. Thus, both hemochromatosis and β-thalassemia patients may benefit from therapies based on preventing iron absorption, such as *Tmprss6*-ASOs. While we were finalizing this manuscript, Schmidt et al. reported another approach to downregulating *Tmprss6* with siRNA (59). *Tmprss6*-siRNA reduced hepatic *Tmprss6* and resulted in effects similar to those reported here, supporting the idea that reduction of *Tmprss6* in the liver is adequate for therapeutic benefit. Future studies will evaluate whether *Tmprss6*-ASO treatment might be comparable or superior to well-established therapies, including iron chelators and phlebotomy. It will also be of interest to study whether *Tmprss6*-ASO treatment may have an additive or synergistic effect in combination with these therapies.

Methods

Generation of ASO. All oligonucleotides used in these studies were 20 nucleotides in length and chemically modified with phosphorothioate in the backbone, 5 2′-*O*-methoxyethyl residues at each terminus, and a central deoxynucleotide region of 10 residues (5-10-5 gapmer). Oligonucleotides were synthesized using an Applied Biosystems 380B automated DNA synthesizer (PerkinElmer Life and Analytical Sciences–Applied Biosystems) and purified as previously described (36). Sequence were as follows: ASO#1, 5′-GCTTAGAGTACAGCCCACTT-3′; ASO#2, 5′-TTTCTTTCCTACAGAGACCC-3′. ASOs were dissolved in PBS (Ca-Mg; Invitrogen) for in vivo experiments.

Culture of hepatocytes and treatment with ASO. Mouse primary hepatocytes were prepared using the standard collagenase procedure described previously (60). Electroporation of ASOs was carried out using the HT-200 BTX Electroporator with the ElectroSquare Porator (ECM 830) voltage source in 96-well electroporation plates (BTX, 2 mm; Harvard Apparatus). Cells were harvested 16 hours after electroporation. Cells were electroporated in the presence of *Tmprss6*-ASOs at the indicated concentrations and plated. Sixteen hours after transfection, total cellular RNA was isolated, and the amount of *Tmprss6* mRNA was quantified using a quantitative RT-PCR (qRT-PCR) assay (TaqMan).

Generation and treatment of Hfe$^{-/-}$ and thalassemic mice. *Hfe$^{-/-}$* and *th3/+* mice, all on the C57BL/6 background, were bred, respectively, at Jackson Laboratory and the mouse facility of Weill Cornell Medical College. Pathological analysis of tissues was as previously described (29). Animals were treated with either vehicle control (PBS), *Tmprss6*-ASO, or control ASO by subcutaneous injections twice a week for the indicated duration. Animals were sacrificed 2 days after the final dose for analyses.

Hematological studies. Blood samples were obtained by retroorbital puncture under anesthesia. CBCs were measured on an Advia 120 analyzer (H-System; Bayer Corp.).

Measurement of tissue iron content, serum parameters. Serum parameters (iron, Tf, ferritin, UIBC, bilirubin) were measured on the AU480 Clinical Analyzer (Beckman Coulter). Serum EPO was analyzed with an ELISA kit following manufacturer's instructions. Tissue iron content was assayed at Exova (Santa Fe Springs) for WT and *Hfe$^{-/-}$* mice, and The Diagnostic Center for Population and Animal Health (DCPAH) at Michigan State University (Lansing, Michigan, USA) for *th3/+* mice.

FACS analysis: erythropoiesis, ROS, and apoptosis analyses by flow cytometry. Erythroid cells were analyzed from both the spleen and BM by FACS analysis using the Ter119 and CD44 antibodies. This assay allows the separation of erythroid cells into distinct populations corresponding to proerythroblasts (fraction I), basophilic (II), polychromatic (III), orthochromatic cells, and reticulocytes (IV), and mature rbc (V) (61). BM and spleen cells were incubated with FITC-labeled anti-mouse CD71 and APC-conjugated anti-mouse Ter119 antibodies (BD Biosciences — Pharmingen). In a subset of mice, the cells were stained with a PE-conjugated anti-mouse CD44 marker (BD Biosciences — Pharmingen) and APC-conjugated Ter119. In the peripheral blood and immature erythroid cells from the spleen and BM of these subsets, ROS were detected with the indicator CM-H2DCFDA (Invitrogen). Apoptosis was also detected in the spleen and BM with lactadherin and 7-AAD, according to the instructions provided by the manufacturer. For all the analyses, cells were sorted using a FACSCalibur instrument (BD) and the results analyzed with FlowJo software (Tree Star Inc.).

qPCR. Cultured cells were lysed, and total RNA was extracted with a QIAGEN RNeasy column. Animal tissues were homogenized in a guanidine isothiocyanate solution (Invitrogen) supplemented with 8% 2-mercaptoethanol (Sigma-Aldrich). Total RNA was prepared according to the RNeasy mini kit instructions (QIAGEN). The qRT-PCR analyses were done using an ABI Prism 7700 sequence detector (Applied Biosystems). The sequences of primers and probe used were as follows: *Tmprss6*: forward: 5′-ATTCCACGCTGGGCTGTTAT-3′, reverse: 5′-CTGGTCAGGCCCCTTCAA-3′, probe: 5′-Fam-TGAACCCAGGCCAGGTCCTCCC-Tamra-5′; *Hamp*: forward: 5′-TGCAGAAGAGAAGGAAGAGAGACA-3′, reverse: 5′-CACACTGGGAATTGTTACAGCATT-3′, probe: 5′-Fam-CAACTTCCCCATCTGCATCTTCTGCTGT-Tamra-5′. Additional oligonucleotide sequences are indicated in Supplemental Table 3. PCR results were normalized to total RNA measure by Quant-iT RiboGreen RNA Reagent (Molecular Probes).

Analyses of α- and β-globin chains in plasma and on rbc membranes. To visualize soluble as well as membrane-bound globins, we utilized TAU gel electrophoresis, which resolves α- and β-globin subunits under denaturing conditions (19, 30). The fraction of sample loaded on the TAU gel was adjusted relative to the number of rbc from CBC, so that the same number of erythrocytes is represented in each lane.

Statistics. Data are presented as mean ± SD. Unpaired 2-tailed Student's *t* test was performed using Microsoft Excel, Mac 2008, software. $P < 0.05$ was considered statistically significant.

Study approval. All the animal studies were conducted under protocols approved by the Institutional Animal Care and Use Committee (IACUC) of Weill Cornell Medical College and Isis Pharmaceuticals.

Acknowledgments

This work is supported by the Children's Cancer and Blood Foundation, NIH grant NIDDK-1R01DK090554, and Isis Pharmaceuticals (to S. Rivella). S. Rivella is also a consultant for Isis Pharmaceuticals. The authors would like to thank Tracy Reigle for her help with formatting the figures.

Received for publication October 10, 2012, and accepted in revised form January 17, 2013.

Address correspondence to: Brett P. Monia, Isis Pharmaceuticals, 2855 Gazelle Ct., Carlsbad, California 92010, USA. Phone: 760.603.2350; Fax: 760.603.2502; E-mail: bmonia@isisph.com. Or to: Stefano Rivella, Weill Cornell Medical College, 515 East 71st St. S702, New York, New York 10021, USA. Phone: 212.746.4941; Fax: 212.746.8423; E-mail: str2010@med.cornell.edu.

1. Andrews NC. Disorders of iron metabolism. *N Engl J Med*. 1999;341(26):1986–1995.
2. Nemeth E, Ganz T. Regulation of iron metabolism by hepcidin. *Annu Rev Nutr*. 2006;26:323–342.
3. Zhang AS, Enns CA. Molecular mechanisms of normal iron homeostasis. *Hematology Am Soc Hematol Educ Program*. 2009;2009(1):207–214.
4. Ganz T, Nemeth E. Hepcidin and disorders of iron metabolism. *Annu Rev Med*. 2011;62:347–360.
5. Krause A, et al. LEAP-1, a novel highly disulfide-bonded human peptide, exhibits antimicrobial activity. *FEBS Lett*. 2000;480(2–3):147–150.

6. Park CH, Valore EV, Waring AJ, Ganz T. Hepcidin, a urinary antimicrobial peptide synthesized in the liver. *J Biol Chem*. 2001;276(11):7806–7810.
7. Gardenghi S, Grady RW, Rivella S. Anemia, ineffective erythropoiesis, and hepcidin: interacting factors in abnormal iron metabolism leading to iron overload in β-thalassemia. *Hematol Oncol Clin North Am*. 2010;24(6):1089–1107.
8. Ginzburg Y, Rivella S. beta-thalassemia: a model for elucidating the dynamic regulation of ineffective erythropoiesis and iron metabolism. *Blood*. 2011; 118(16):4321–4330.
9. Nemeth E, et al. Hepcidin regulates cellular iron efflux by binding to ferroportin and inducing its internalization. *Science*. 2004;306(5704):2090–2093.
10. Babitt JL, et al. Bone morphogenetic protein signaling by hemojuvelin regulates hepcidin expression. *Nat Genet*. 2006;38(5):531–539.
11. Andriopoulos B, et al. BMP6 is a key endogenous regulator of hepcidin expression and iron metabolism. *Nat Genet*. 2009;41(4):482–487.
12. Steinbicker AU, et al. Perturbation of hepcidin expression by BMP type I receptor deletion induces iron overload in mice. *Blood*. 2011;118(15):4224–4230.
13. Huang FW, Pinkus JL, Pinkus GS, Fleming MD, Andrews NC. A mouse model of juvenile hemochromatosis. *J Clin Invest*. 2005;115(8):2187–2191.
14. Niederkofler V, Salie R, Arber S. Hemojuvelin is essential for dietary iron sensing, and its mutation leads to severe iron overload. *J Clin Invest*. 2005; 115(8):2180–2186.
15. Zhang AS, Gao J, Koeberl DD, Enns CA. The role of hepatocyte hemojuvelin in the regulation of bone morphogenic protein-6 and hepcidin expression in vivo. *J Biol Chem*. 2010;285(22):16416–16423.
16. Du X, et al. The serine protease TMPRSS6 is required to sense iron deficiency. *Science*. 2008; 320(5879):1088–1092.
17. Silvestri L, Pagani A, Nai A, De Domenico I, Kaplan J, Camaschella C. The serine protease matriptase-2 (TMPRSS6) inhibits hepcidin activation by cleaving membrane hemojuvelin. *Cell Metab*. 2008;8(6):502–511.
18. Finberg KE, et al. Mutations in TMPRSS6 cause iron-refractory iron deficiency anemia (IRIDA). *Nat Genet*. 2008;40(5):569–571.
19. Finberg KE, Whittlesey RL, Fleming MD, Andrews NC. Down-regulation of Bmp/Smad signaling by Tmprss6 is required for maintenance of systemic iron homeostasis. *Blood*. 2010;115(18):3817–3826.
20. Maxson JE, Chen J, Enns CA, Zhang AS. Matriptase-2- and proprotein convertase-cleaved forms of hemojuvelin have different roles in the down-regulation of hepcidin expression. *J Biol Chem*. 2010; 285(50):39021–39028.
21. Vujic Spasic M, et al. Hfe acts in hepatocytes to prevent hemochromatosis. *Cell Metab*. 2008; 7(2):173–178.
22. Feder JN, et al. A novel MHC class I-like gene is mutated in patients with hereditary haemochromatosis. *Nat Genet*. 1996;13(4):399–408.
23. Ramos P, et al. Enhanced erythropoiesis in Hfe-KO mice indicates a role for Hfe in the modulation of erythroid iron homeostasis. *Blood*. 2011; 117(4):1379–1389.
24. Brissot P. [Haemochromatoses. New understanding, new treatments]. *Gastroenterol Clin Biol*. 2009; 33(8–9):859–867.
25. Rivella S. The role of ineffective erythropoiesis in non-transfusion-dependent thalassemia. *Blood Rev*. 2012;26(suppl 1):S12–S15.
26. Gardenghi S, et al. Increased hepcidin expression in mice affected by β-thalassemia reduces iron overload with no effect on anemia. *Blood*. 2008;112(1):53.
27. Libani IV, et al. Decreased differentiation of erythroid cells exacerbates ineffective erythropoiesis in beta-thalassemia. *Blood*. 2008;112(3):875–885.
28. Rivella S. Ineffective erythropoiesis and thalassemias. *Curr Opin Hematol*. 2009;16(3):187–194.
29. Gardenghi S, et al. Hepcidin as a therapeutic tool to limit iron overload and improve anemia in beta-thalassemic mice. *J Clin Invest*. 2010;120(12):4466–4477.
30. Parrow NL, Gardenghi S, Rivella S. Prospects for a hepcidin mimic to treat beta-thalassemia and hemochromatosis. *Expert Rev Hematol*. 2011;4(3):233–235.
31. Finberg KE, Whittlesey RL, Andrews NC. Tmprss6 is a genetic modifier of the Hfe-hemochromatosis phenotype in mice. *Blood*. 2011;117(17):4590–4599.
32. Nai A, et al. Deletion of TMPRSS6 attenuates the phenotype in a mouse model of beta-thalassemia. *Blood*. 2012;119(21):5021–5029.
33. Kautz L, et al. Iron regulates phosphorylation of Smad1/5/8 and gene expression of Bmp6, Smad7, Id1, and Atoh8 in the mouse liver. *Blood*. 2008; 112(4):1503–1509.
34. Parrow NL, et al. Decreased hepcidin expression in murine beta-thalassemia is associated with suppression of Bmp/Smad signaling. *Blood*. 2012; 119(13):3187–3189.
35. Frazer DM, Wilkins SJ, Darshan D, Badrick AC, McLaren GD, Anderson GJ. Stimulated erythropoiesis with secondary iron loading leads to a decrease in hepcidin despite an increase in bone morphogenetic protein 6 expression. *Br J Haematol*. 2012; 157(5):615–626.
36. Bennett CF, Swayze EE. RNA targeting therapeutics: molecular mechanisms of antisense oligonucleotides as a therapeutic platform. *Annu Rev Pharmacol Toxicol*. 2010;50:259–293.
37. Enns CA, Ahmed R, Zhang AS. Neogenin interacts with matriptase-2 to facilitate hemojuvelin cleavage. *J Biol Chem*. 2012;287(42):35104–35117.
38. Wood AD, et al. ID1 promotes expansion and survival of primary erythroid cells and is a target of JAK2V617F-STAT5 signaling. *Blood*. 2009; 114(9):1820–1830.
39. Tanno T, et al. High levels of GDF15 in thalassemia suppress expression of the iron regulatory protein hepcidin. *Nat Med*. 2007;13(9):1096–1101.
40. Hooper JD, Campagnolo L, Goodarzi G, Truong TN, Stuhlmann H, Quigley JP. Mouse matriptase-2: identification, characterization and comparative mRNA expression analysis with mouse hepsin in adult and embryonic tissues. *Biochem J*. 2003; 373(pt 3):689–702.
41. Casanovas G, et al. The murine growth differentiation factor 15 is not essential for systemic iron homeostasis in phlebotomized mice. *Haematologica*. 2013;98(3):444–447.
42. Feder JN, et al. The hemochromatosis founder mutation in HLA-H disrupts beta2-microglobulin interaction and cell surface expression. *J Biol Chem*. 1997;272(22):14025–14028.
43. Porto G, da Silva BM, Vincente C, de Sousa M. Idiopathic haemochromatosis in north Portugal: association with haplotype A3B7. *J Clin Pathol*. 1989;42(6):667–668.
44. Brissot P, de Bels F. Current approaches to the management of hemochromatosis. *Hematology Am Soc Hematol Educ Program*. 2006;2006(1):36–41.
45. Gan EK, Powell LW, Olynyk JK. Natural history and management of HFE-hemochromatosis. *Semin Liver Dis*. 2011;31(3):293–301.
46. Nemeth E, Ganz T. The role of hepcidin in iron metabolism. *Acta Haematol*. 2009;122(2–3):78–86.
47. Centers for Disease Control and Prevention. Hemochromatosis (Iron Storage Disease). CDC Web site. http://www.cdc.gov/ncbddd/hemochromatosis/training/treatment/monitoring_treatment.html. Updated September 23, 2010. Accessed February 11, 2013.
48. Weatherall DJ. The definition and epidemiology of non-transfusion-dependent thalassemia. *Blood Rev*. 2012;26(suppl 1):S3–S6.
49. Taher AT, Musallam KM, Karimi M, Cappellini MD. Contemporary approaches to treatment of beta-thalassemia intermedia. *Blood Rev*. 2012; 26(suppl 1):S24–S27.
50. Taher AT, Cappellini MD, Musallam KM. Recent advances and treatment challenges in patients with non-transfusion-dependent thalassemia. *Blood Rev*. 2012;26(suppl 1):S1–S2.
51. Roy CN, Mak HH, Akpan I, Losyev G, Zurakowski D, Andrews NC. Hepcidin antimicrobial peptide transgenic mice exhibit features of the anemia of inflammation. *Blood*. 2007;109(9):4038–4044.
52. Corradini E, et al. BMP6 treatment compensates for the molecular defect and ameliorates hemochromatosis in Hfe knockout mice. *Gastroenterology*. 2010;139(5):1721–1729.
53. Preza GC, et al. Minihepcidins are rationally designed small peptides that mimic hepcidin activity in mice and may be useful for the treatment of iron overload. *J Clin Invest*. 2011;121(12):4880–4888.
54. Ramos E, et al. Minihepcidins prevent iron overload in a hepcidin-deficient mouse model of severe hemochromatosis. *Blood*. 2012;120(18):3829–3836.
55. Li H, et al. Transferrin therapy ameliorates disease in beta-thalassemic mice. *Nat Med*. 2010;16(2):177–182.
56. Cox LA, Adrian GS. Posttranscriptional regulation of chimeric human transferrin genes by iron. *Biochemistry*. 1993;32(18):4738–4745.
57. Ponka P, Beaumont C, Richardson DR. Function and regulation of transferrin and ferritin. *Semin Hematol*. 1998;35(1):35–54.
58. Morton AG, Tavill AS. The control of hepatic iron uptake: correlation with transferring synthesis. *Br J Haematol*. 1978;39(4):497–507.
59. Schmidt PJ, et al. An RNAi therapeutic targeting Tmprss6 decreases iron overload in *Hfe*$^{-/-}$ mice and ameliorates anemia and iron overload in murine beta-thalassemia intermedia. *Blood*. 2013; 121(7):1200–1208.
60. Quistorff B, Dich J, Grunnet N. Preparation of isolated rat liver hepatocytes. *Methods Mol Biol*. 1990;5:151–160.
61. Chen K, Liu J, Heck S, Chasis JA, An X, Mohandas N. Resolving the distinct stages in erythroid differentiation based on dynamic changes in membrane protein expression during erythropoiesis. *Proc Natl Acad Sci U S A*. 2009;106(41):17413–17418.